Photo Injector Test facility at DESY, Zeuthen site.

Space charge dominated photoemission at PITZ

Mikhail Krasilnikov (DESY) for the PITZ Team

European Workshop on Photocathodes for Particle Accelerator Applications / EWPAA 2017
20-22.09.2017, Helmholtz-Zentrum Berlin, Germany

HELMHOLTZ | ASSOCIATION

DESY

Photo Injector Test facility at DESY, Zeuthen site (PITZ)

PITZ ➔ development, test and optimization of high brightness electron sources for sc linac driven FELs:

⇒ test-bed for FEL injectors: FLASH, the European XFEL (gun cavities and subsystems, e.g. photocathode laser)

⇒ **High brightness → small** $\varepsilon_{x,y}$ (projected and slice)

⇒ further studies → e.g. **photocathodes (PC)**: dark current, **photoemission**, QE, thermal emittance, …

+ detailed comparison with simulations = benchmarking for the PI physics

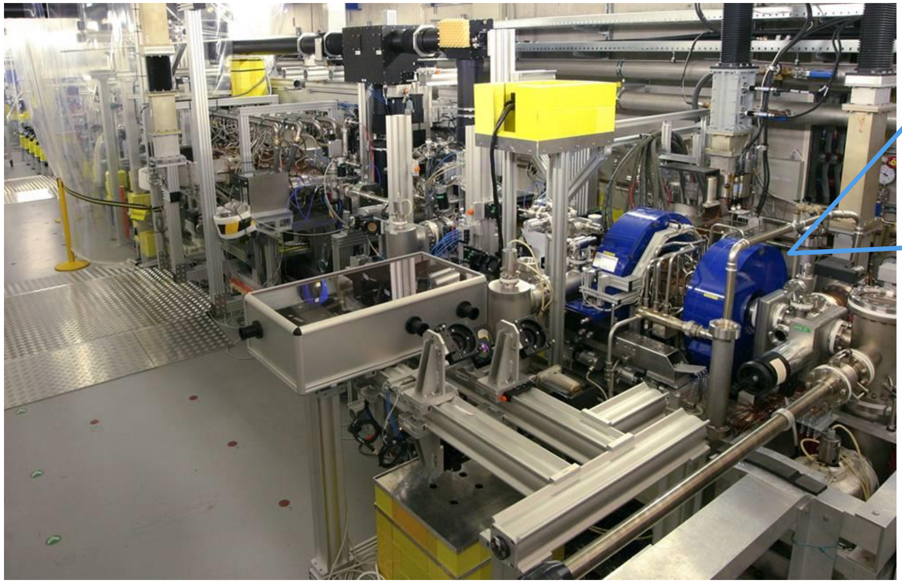

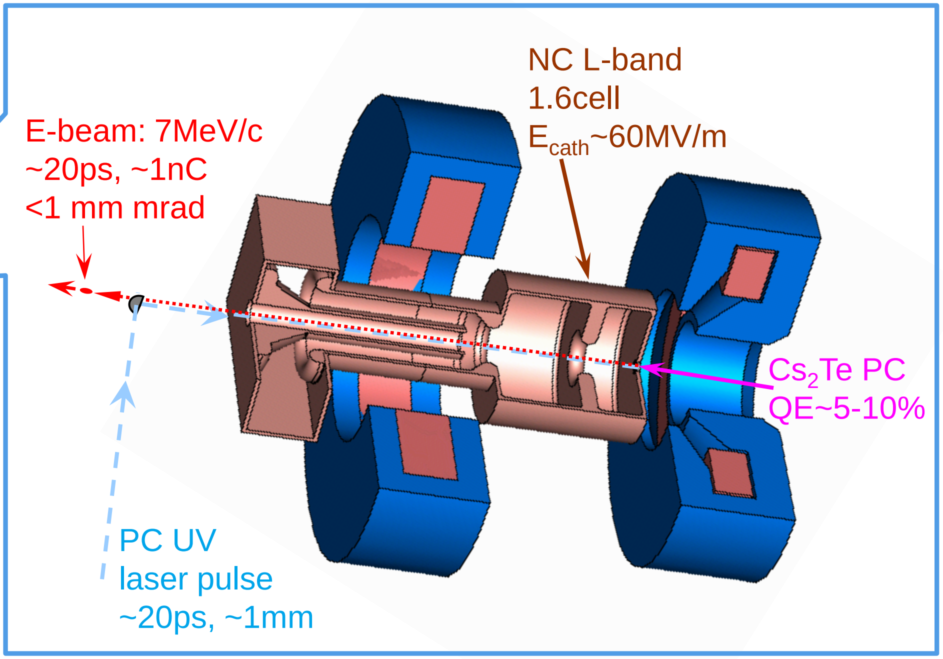

PITZ: Simulations versus Measurements

Asymmetry → kick?

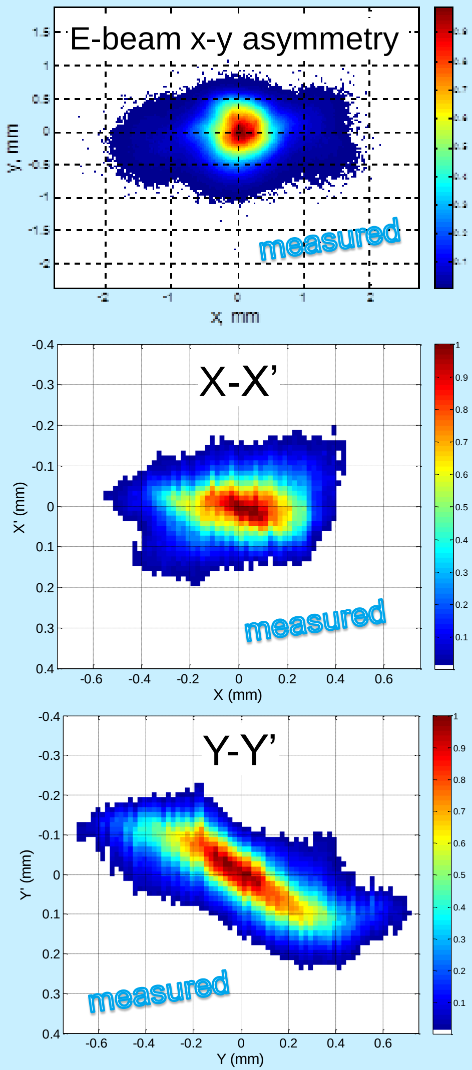

Space charge

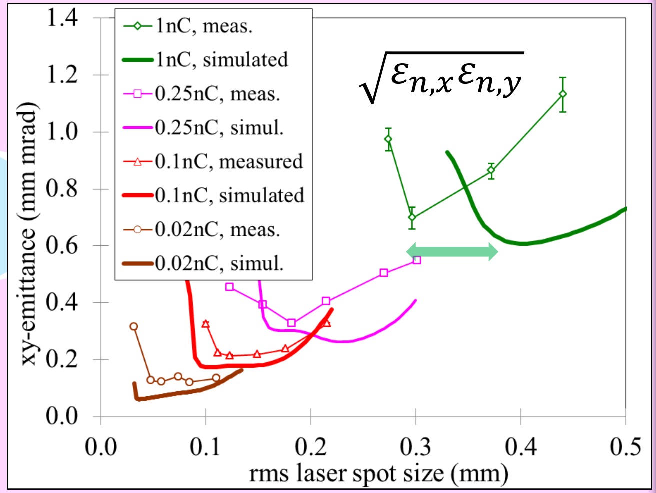

M. Krasilnikov et al., PRSTAB 15, 100701, 2012.

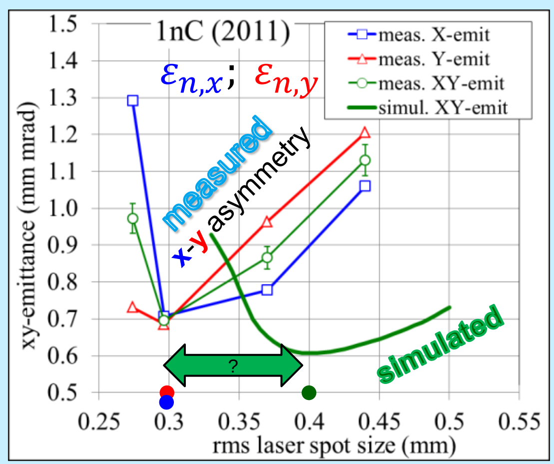

Charge production

Photocathode laser

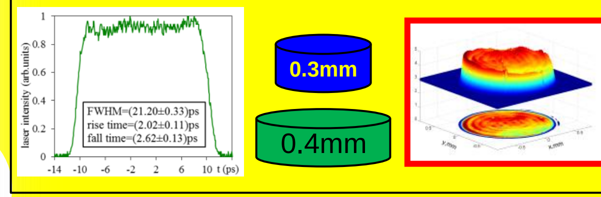

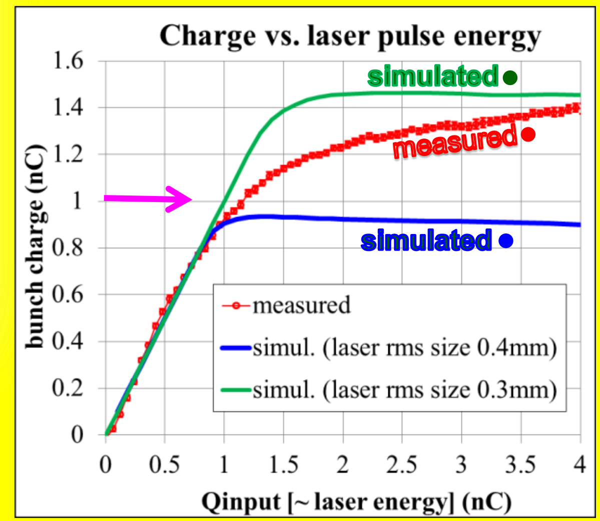

<u>Experimental emittance minimization</u>: optimum PC laser spot size (space charge density) ➔ **transition**: linear (QE-limited) to saturated (SC limited) regime

Photoemission: impact of RF gradient and laser pulse temporal profile

Experiment ➔ Emission curves: bunch charge $Q(\boldsymbol{E_{cath}}, \varphi_0^{MMMG}, E_{laser}, \boldsymbol{Laser\ temporal\ profile})$

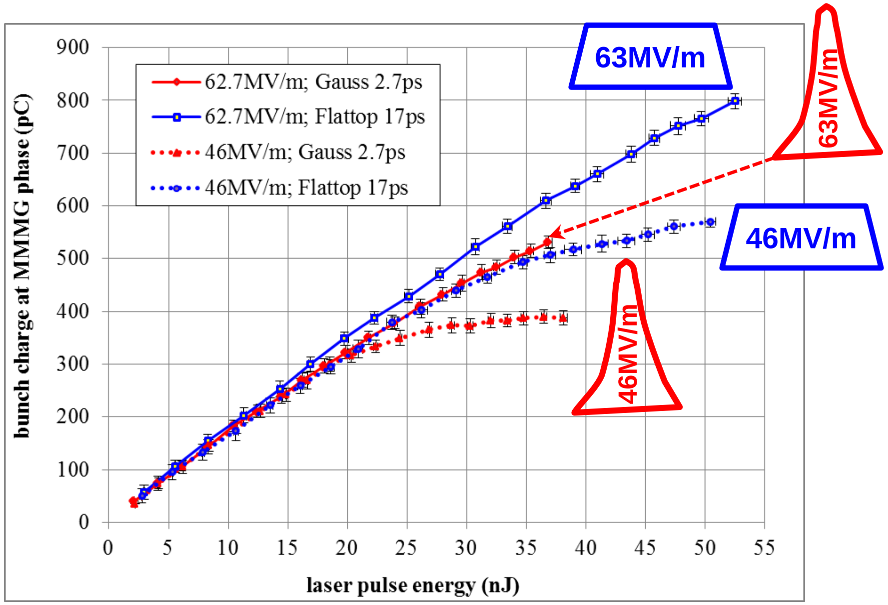

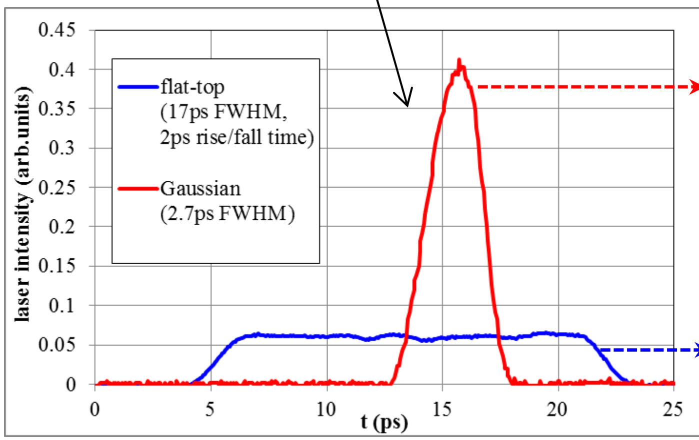

Transverse

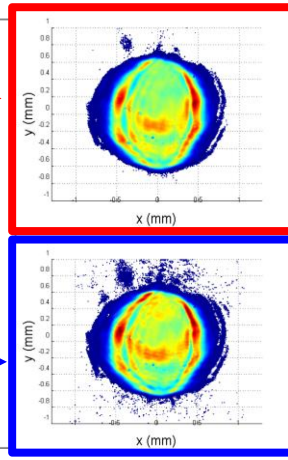

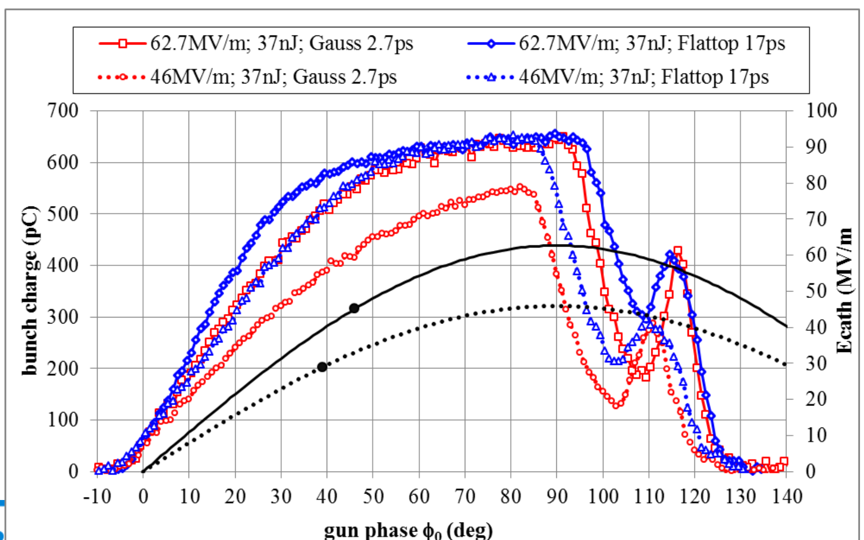

From the parallel plate capacitor (sheet beam) model:

$Q_{SC-lim} = \pi\varepsilon_0 R^2 E_0 \sin\varphi_0 = \pi\varepsilon_0 R^2 E_{cath}$

E.g. for $E_{cath} = 50\frac{MV}{m}; R = 0.6mm;$

$\boldsymbol{Q_{QE-lim,PPCM} \cong 500pC}$ **<< observed!!!**

Photoemission depends on:

- Ecath → **Schottky**(like) effect
- Laser pulse duration → space charge effect
- Emission curves $Q(E_{laser})$ saturate weaker

Photoemission: laser transverse halo modeling

Laser transverse distribution:
Core + Halo model (C+H)

$$F_l(r) = \frac{E_l}{\pi R_c^2 + 2\pi\xi{\sigma_r}^2}\begin{cases} 1, & if\ \ r \le R_c \\ \xi e^{\frac{R_c^2 - r^2}{2\sigma_r^2}}, & if\ r > R_c \end{cases}$$

Laser radial profile

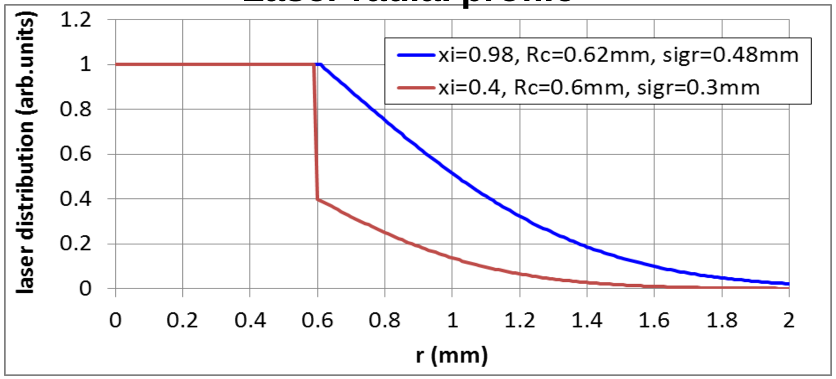

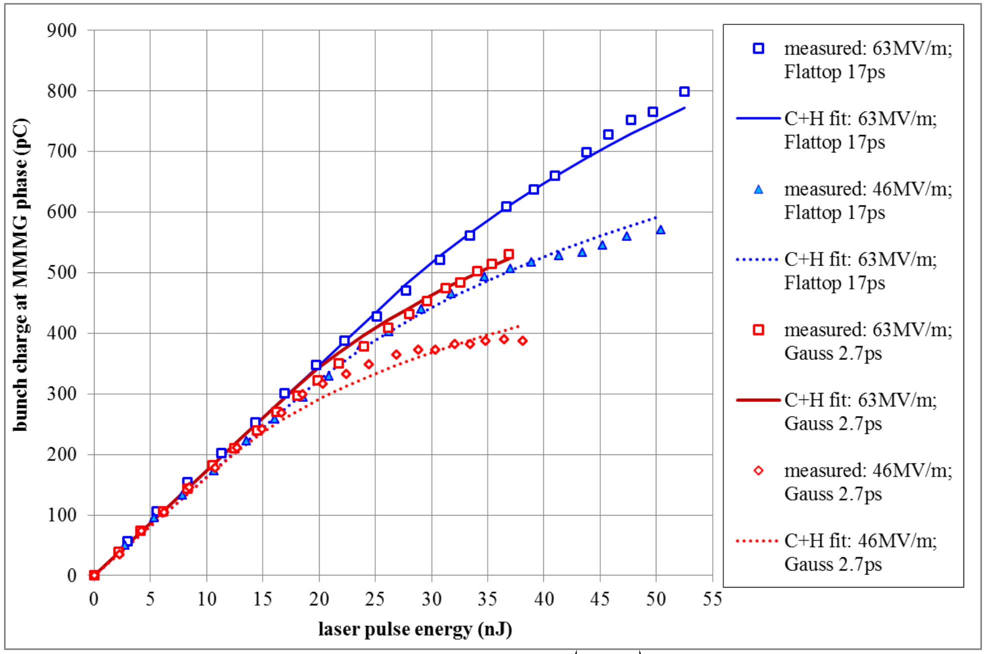

$$\boldsymbol{Q = Q_{core} + Q_{halo}}$$

$$Q_{core} = \frac{1}{1+\xi\cdot\eta}\begin{cases} Q_{exp}, & if\ \ Q_{exp} \le Q_{max} \\ Q_{max} & if\ \ Q_{exp} > Q_{max} \end{cases}$$

$$Q_{halo} = \frac{\eta}{1+\xi\cdot\eta}\begin{cases} \xi\cdot Q_{exp}, & if\ \ \xi\cdot Q_{exp} \le Q_{max} \\ Q_{max}\cdot\left(1+\ln\frac{\xi\cdot Q_{exp}}{Q_{max}}\right) & if\ \ \xi\cdot Q_{exp} > Q_{max} \end{cases}$$

$$Q_{max} = \rho_{scl}\cdot\left(\pi R_c^2 + 2\pi\xi{\sigma_r}^2\right)$$

$$\frac{\rho_{scl}(flat-top)}{\rho_{scl}(Gaussian)} \approx 1.51$$

SC

Cathode laser pulse length (FWHM) ratio ~6

C+H → charge exceed

Core + Halo Model applied to ASTRA simulations

If a uniform distribution is used instead, the charge saturates

Laser radial distribution image

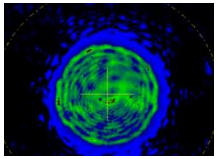

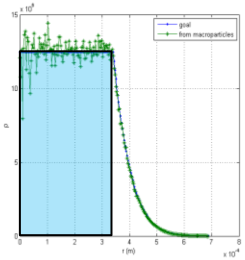

Transverse radial profile core + halo

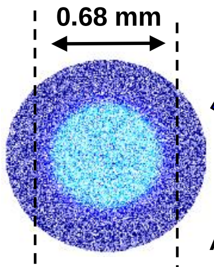

Generated ASTRA input distribution core + halo

Extracted charge with core + halo for 0.8 mm beam diameter with 1.5 ps rms Gaussian temporal at maximum cathode field (ϕ_0=90º)

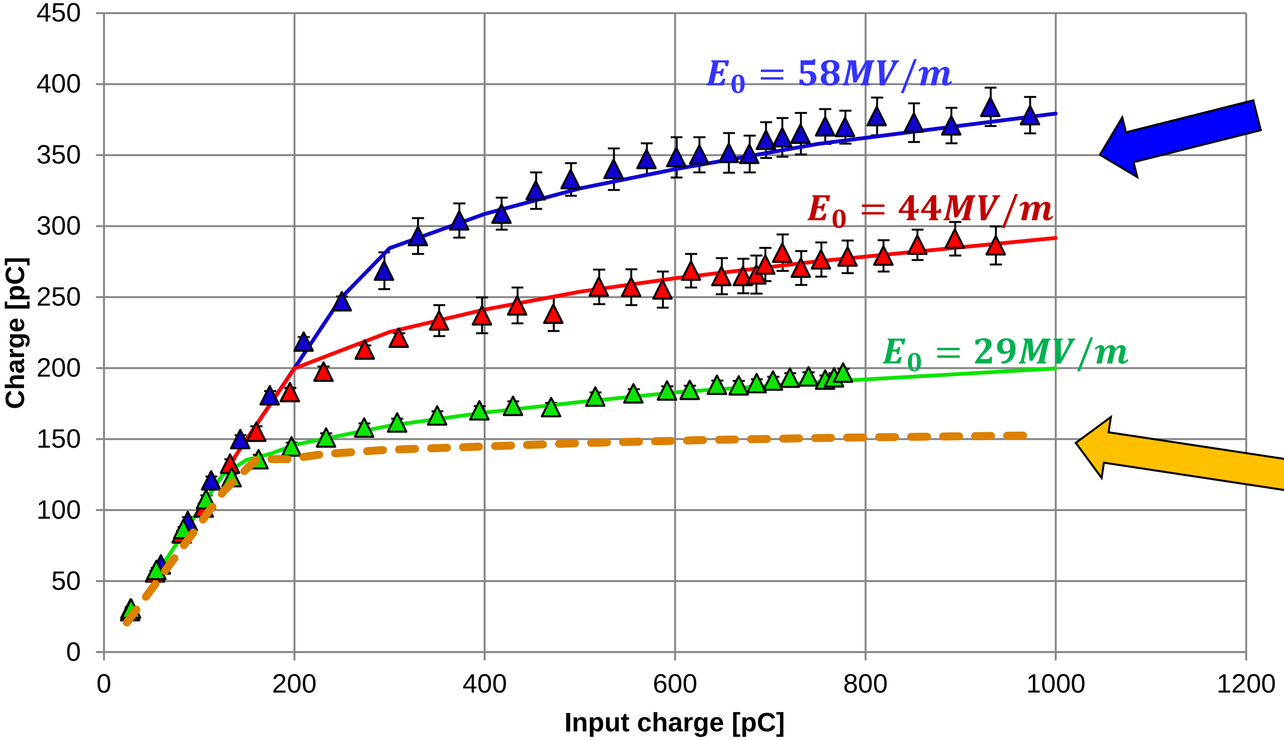

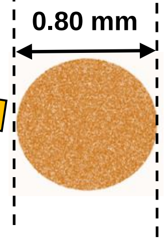

Nominal ASTRA input uniform distribution

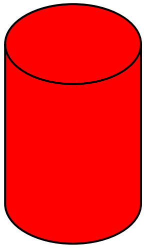

Nominal transverse uniform radial profile

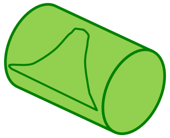

C. Hernandez-Garcia et al., NIM A 871 (2017) 97–104

ASTRA simulations for 2011 case using Core+Halo

> BUT for flattop photocathode laser pulses

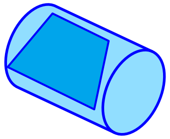

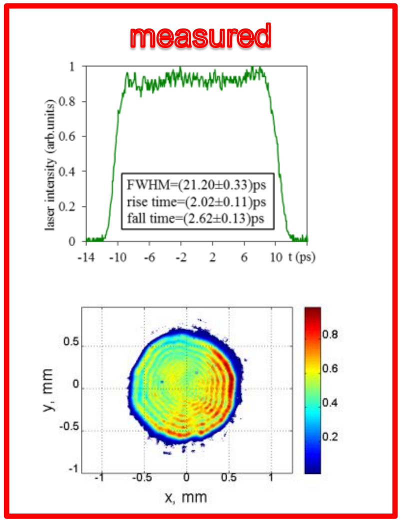

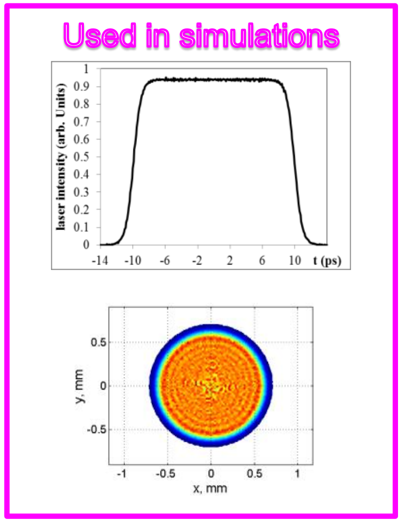

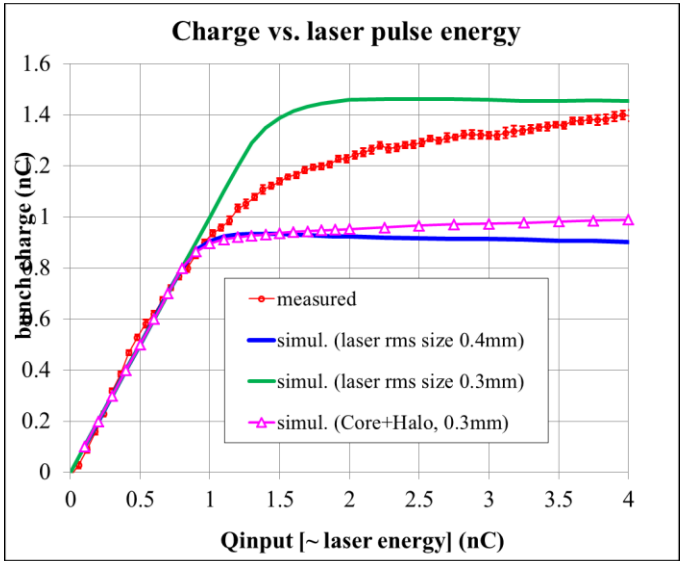

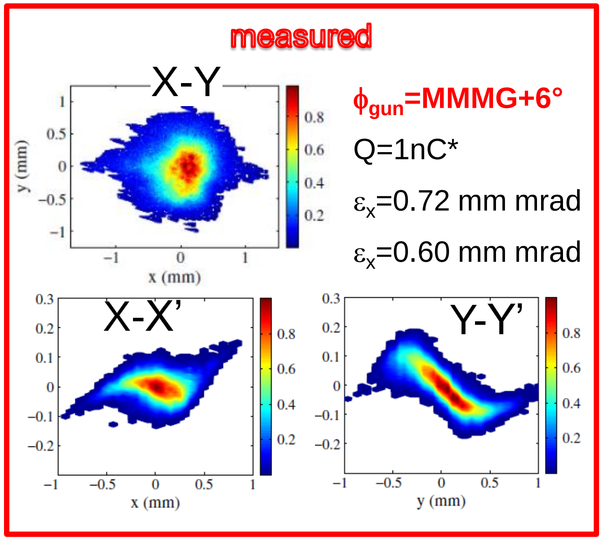

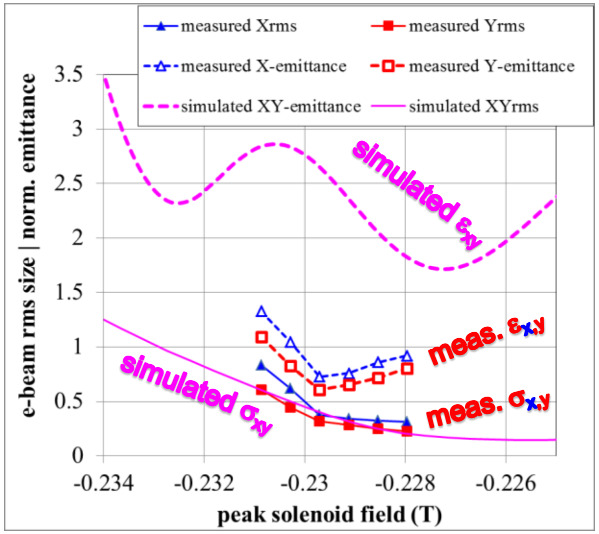

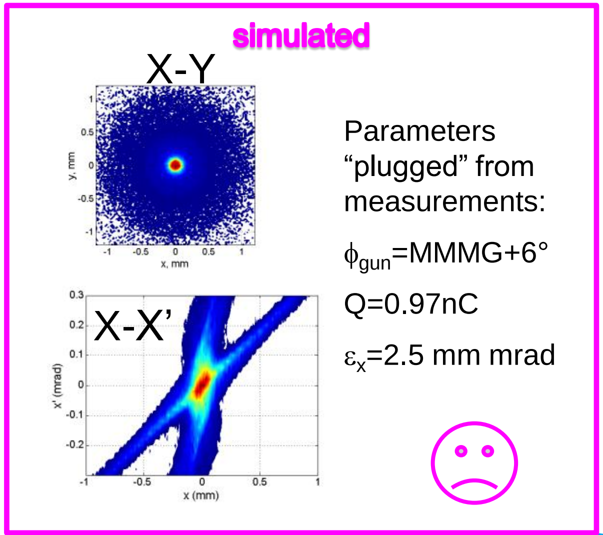

Electron beam X-Y asymmetry studies at PITZ

Possible sources of the beam asymmetry:
- ~~**Vacuum mirror**~~
- ~~**Stray magnetic fields**~~
- ~~**Related to the laser polarization**~~
- ~~**Particular cathode**~~
- **…**
- **RF coupler field asymmetry**
- **Solenoid imperfections (anomalous quadrupole fields)**

Larmor angle experiment

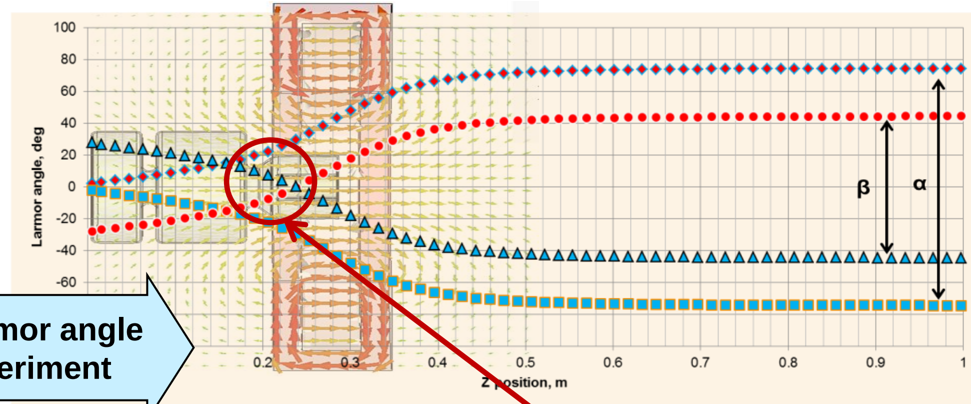

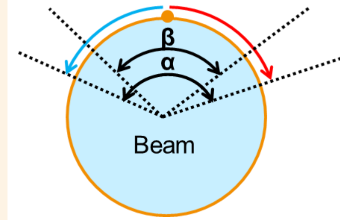

Main solenoid $max[B_z]$, (I_{main} for meas.)	Laser X-Y distribution at cathode			Electron beam X-Y distribution simulated at z=0.18 m	E-beam X-Y distribution at z=5.277 m	
	Measured at VC2	Used in simulations			Simulated	Measured at EMSY1
-0.2087T (-360A) opposite polarity	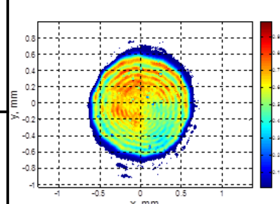	Core + Halo 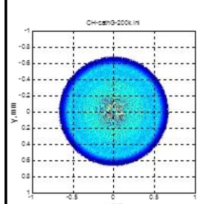	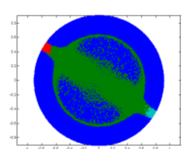	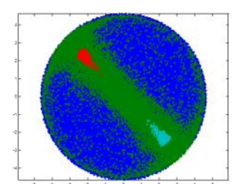	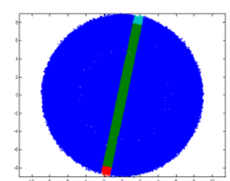	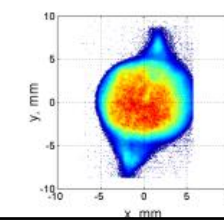
+0.2087T (+360A) normal polarity			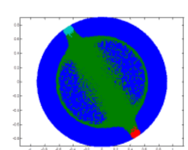	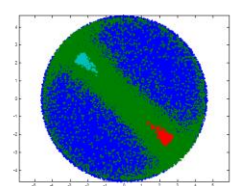	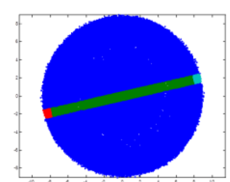	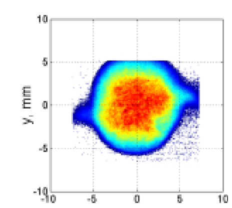

?45° Kick at z~0.2m → skew quadrupole?

Electron beam X-Y asymmetry compensation with gun quads

measured

(0.5nC, Gaussian photocathode laser pulse)

Electron beam measurements **without** gun quadrupoles

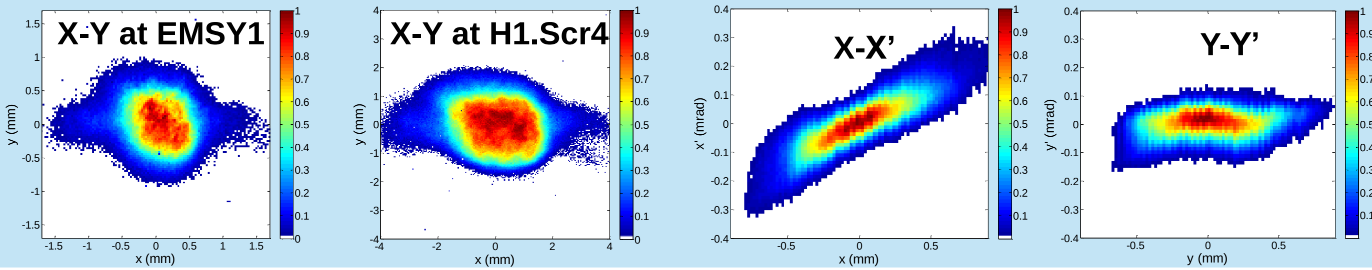

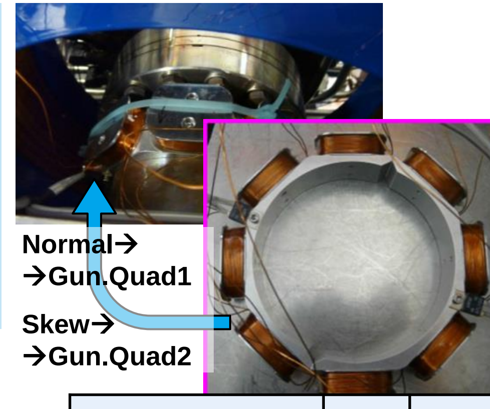

($I_{Gun.Quad1}$; $I_{Gun.Quad2}$) scan at EMSY1

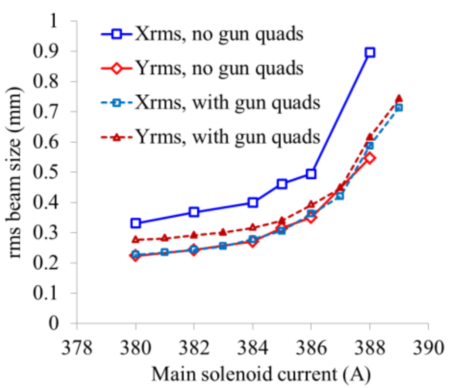

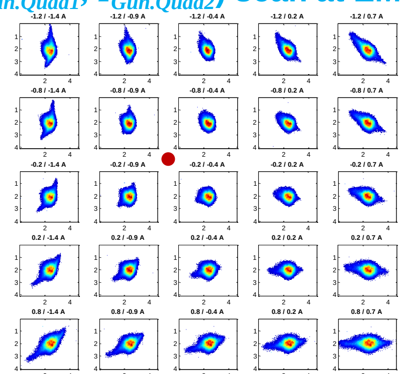

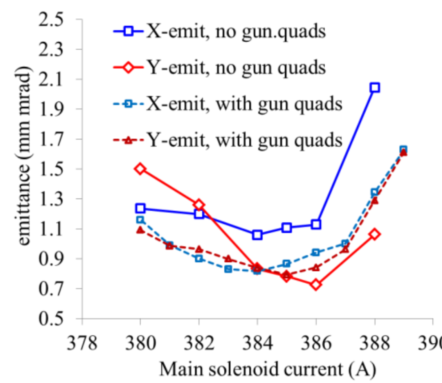

	No gun quads	With gun quads
I_{main}(A)	386	384
$I_{gun.quad1}$ (A)	0	-0.5
$I_{gun.quad2}$ (A)	0	-0.6
σ_x@EMSY1 (mm)	0.50	0.28
σ_y @EMSY1 (mm)	0.35	0.32
$\varepsilon_{x,n}$ (mm mrad)	1.13	0.82
$\varepsilon_{y,n}$ (mm mrad)	0.73	0.84
$\sqrt{\varepsilon_{x,n}\varepsilon_{y,n}}$ (mm mrad)	0.91	0.83
β_x (m)	6.53	3.18
β_y (m)	6.49	3.24
γ_x (mrad)	0.56	0.32
γ_y (mrad)	0.16	0.31

Electron beam measurements **with** gun quadrupoles

($I_{Gun.Quad1}$=-0.6A; $I_{Gun.Quad2}$=-0.5A)

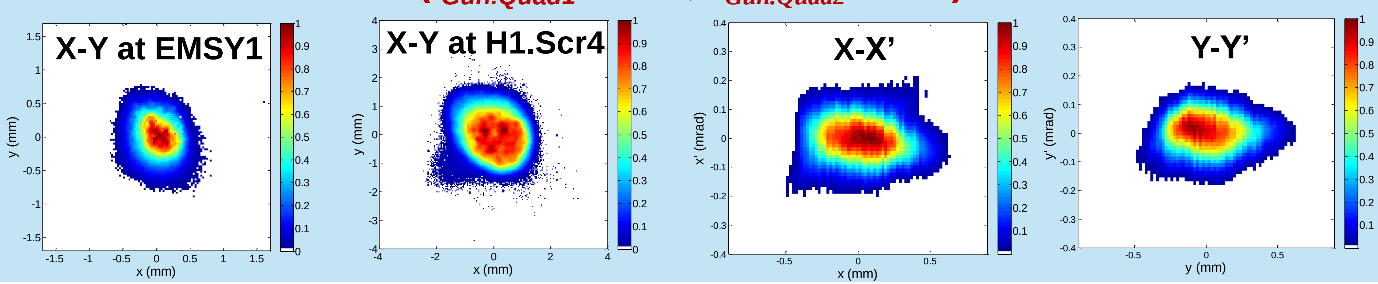

M. Krasilnikov et al.,FEL2017 proceedings, WEP007

ASTRA simulations for Gaussian pulses using Core+Halo

- BUT for flattop photocathode laser pulses

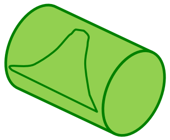

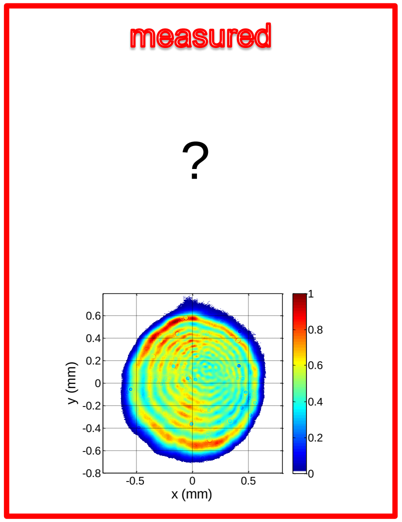

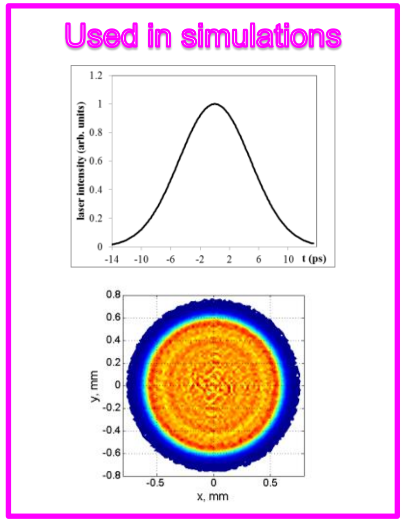

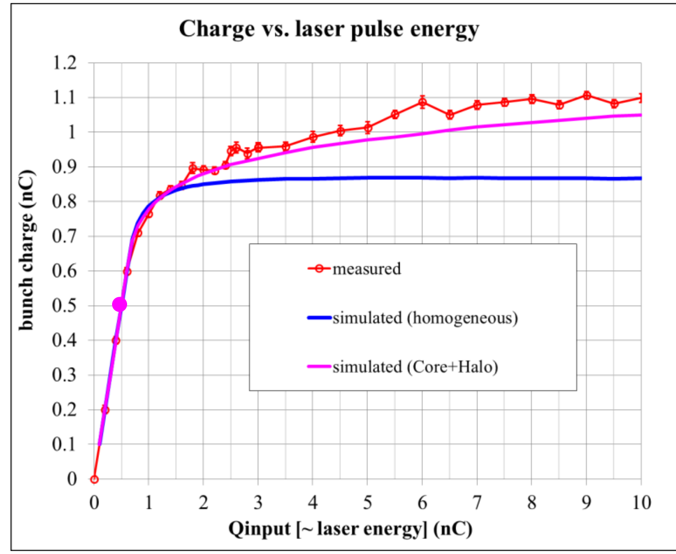

measured

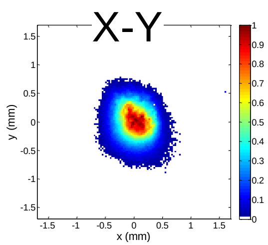

ϕ_{gun}=MMMG

Q=0.5nC

ε_x=0.82 mm mrad

ε_x=0.84 mm mrad

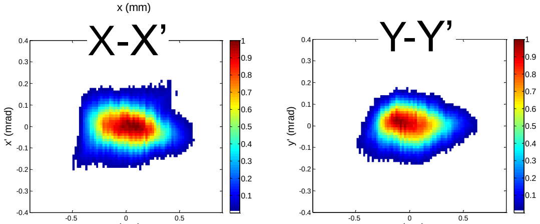

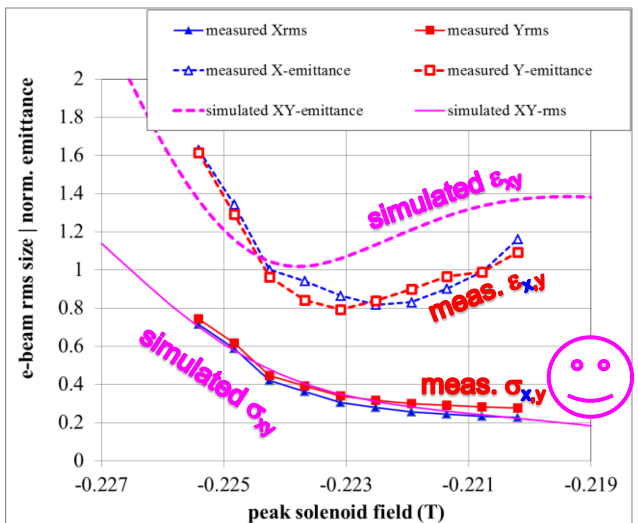

simulated

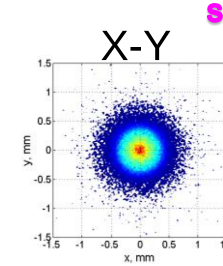

Parameters "plugged" from measurements:

ϕ_{gun}=MMMG

Q=0.5nC

ε_x=1.05 mm mrad

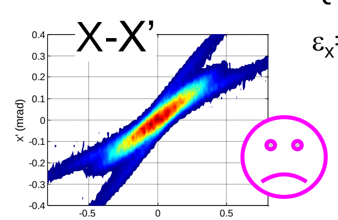

Photoemission from Cs2Te photocathode

Three step model of photoemission:

$$J_{FD*} \propto (\hbar\omega - E_a - E_g)^{\nu}$$

1. **Absorption** of laser photons in bulk material and excitation (isotropically distributed) of photo-e⁻→ factors:
   - reflectivity $R(\omega)$
   - penetration depth $\delta(\omega)$
   - complex dielectric constant $\epsilon(\omega)$
2. **Transport** of excited photoelectrons to surface with inelastic and isotropic scattering → factors:
   - electron energy E
   - scattering rates (relaxation times) $\tau(E)$, mainly *e-p*
   - mean free path $l_{MFP}(E) = \frac{\hbar k(E)}{m^*}\tau(E) \rightarrow \frac{\delta(\omega)}{l_{MFP}(E)}$
   - scattering factor $f_{\lambda}(\cos\theta, E)$
   - "fatal" approximation is less applicable…
3. **Emission** → probability of transport over barrier V_0
   - barrier height E_a (measured from conduction band minimum), band gap E_g
   - escape cone θ_{max}
   - normal energy $E\cos^2\theta$ of photo-e-: $P(E > V_0)$- Heaviside step function of emission probability → Airy function
   - Band bending

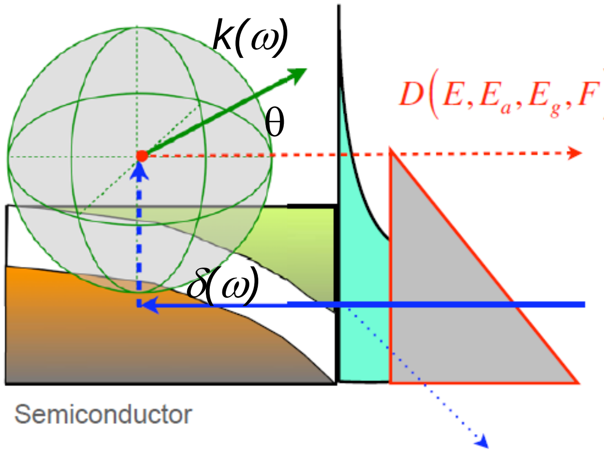

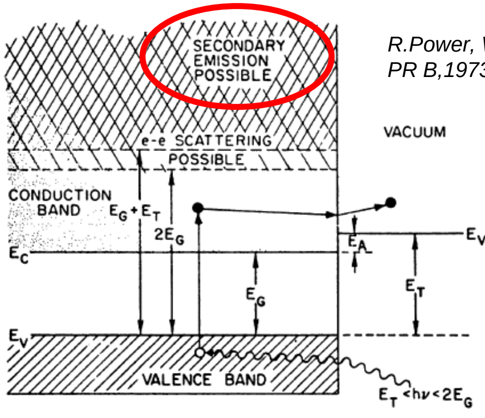

R.Power, W. Spicer et al., PR B,1973 (8)

FIG. 3. Schematic energy-level diagram of a semiconductor photoemitter where $E_G \gg E_A$. The minimum threshold energies for electron-electron scattering ($2E_G$) and for secondary electron emission ($E_G + E_T$) are indicated.

K. L. Jensen "Transfer matrix methods, photoemission and heterostructures", P3 workshop 2016

Photoemission: slice emittance formation

Very short non-relativistic bunch at the cathode → nonlinear Lorentz force

$$E_r(\rho) = \frac{\sigma_0}{4\epsilon_0}\left[\frac{\rho}{r_b} + \frac{3}{8}\left(\frac{\rho}{r_b}\right)^3\right]$$

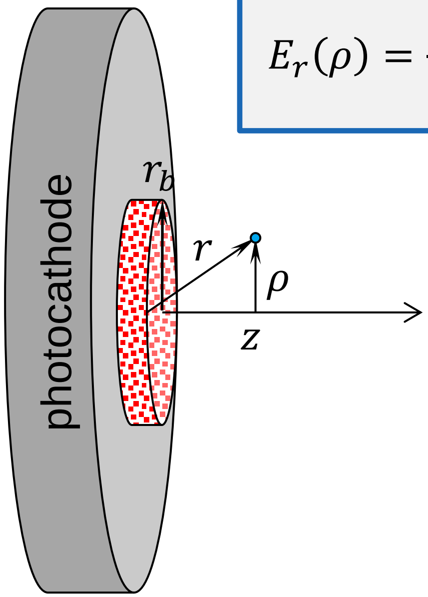

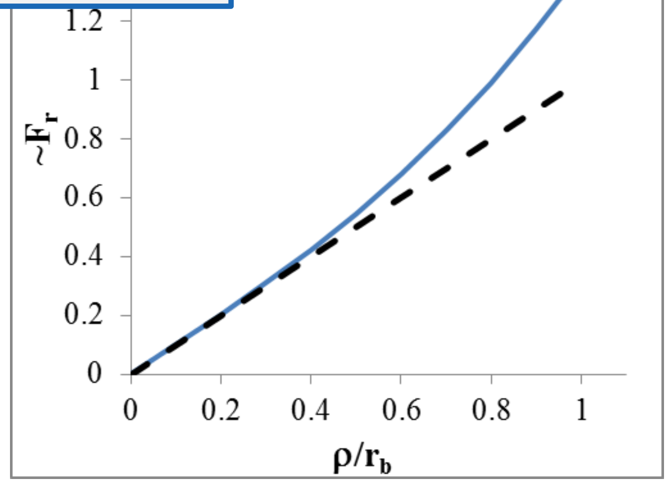

NB: for infinitely long cylinder

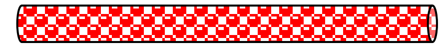

$$E_r(\rho) = \frac{Q/V}{2\epsilon_0}\rho$$

$$F_r(\rho) = \frac{eI\rho}{2\pi\epsilon_0\gamma^2\beta c r_b^2}$$

Space charge term in the envelope equation

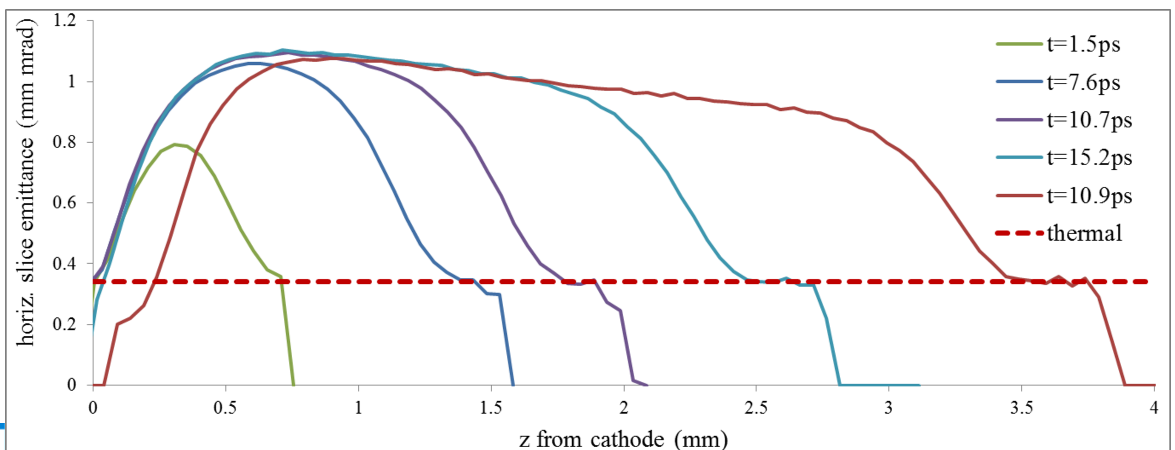

Emission in SC tracking or PIC codes:

- Macroparticle distribution *f(x,y,z=0,t_{start},p_x,p_y,p_z)*
- *Space charge calculation (incl. cath. mirror charge)*
- *Macroparticles reflected back to the cathode (z<0) → lost…*

Photoemission modeling and simulation using a Lienard-Wiechert (LW) approach

➢ Motivation

- **Dynamic generation** of emitted **particle distribution** at cathode
- Flexibilities to **incorporate emission models**
- Taking into account **full electromagnetic fields** (RF + space-charge) during emission
- **Improving the agreement** between measurement and simulation

$$\mathbf{E} = \frac{q}{4\pi\epsilon_0}\left[\frac{(\mathbf{n}-\boldsymbol{\beta})(1-|\boldsymbol{\beta}|^2)}{(1-\boldsymbol{\beta}\cdot\mathbf{n})^3 R^2} + \frac{\mathbf{n}\times(\mathbf{n}-\boldsymbol{\beta})\times\dot{\boldsymbol{\beta}}}{(1-\boldsymbol{\beta}\cdot\mathbf{n})^3 R}\right]\Bigg|_{t=t_r}$$

$$\mathbf{n} = \frac{\mathbf{R}}{|\mathbf{R}|},\ (x-x_r)^2 + (y-y_r)^2 + (z-z_r)^2 = c^2(t-t_r)^2$$

Given N particles' full history to find the EM fields produced by the particles at the observation time

➢ LW Approach with 3D emission process

- **LW solution for the electromagnetic field of a charged particle** in arbitrary motion
- **Full particle trajectory** stored and used for field computation
- Accuracy depends only on **time step** and **number of particles**
- Parallelized PP code

Courtesy Ye Chen

➢ Status of Application

- QE limited regime → OK
- In space charge dominated regime, remaining deviations w.r.t. simulations probably due to:

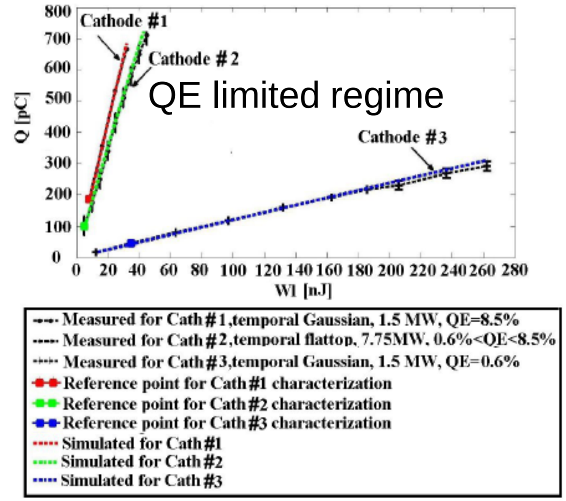

✓Ideal beam distributions initially plugged in the simulations

✓Or/and time dependent work function variation resulting from quantum mechanical effects

- Field-induced work function modification:

$$\Delta\Phi_f(r_\perp,t) = \sqrt{\frac{q^3}{4\pi\varepsilon_0}\left[E_{rf}(r_\perp,t) + E_{sc}(r_\perp,t)\right]}$$

- Charge production per simulation time step:

$$dQ(\mathbf{r}_\perp,t) = \Delta t \iint_S q\frac{P_l(\mathbf{r}_\perp,t)}{h\nu} QE(\mathbf{r}_\perp,t)dS$$

$$QE_J = \frac{(1-R_w)\sqrt{1+\frac{h\nu-\Phi_w}{E_a}}}{2(p_0+1)\left(1+\frac{E_a}{h\nu-\Phi_w}\right)^2}$$

K.L. Jensen, 2007

Some experimental observations
might be related to photoemission issues

Gun-4.6 (PITZ): mean momentum and MMMG phase

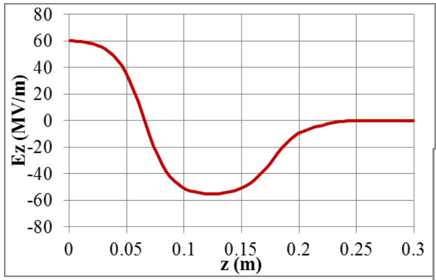

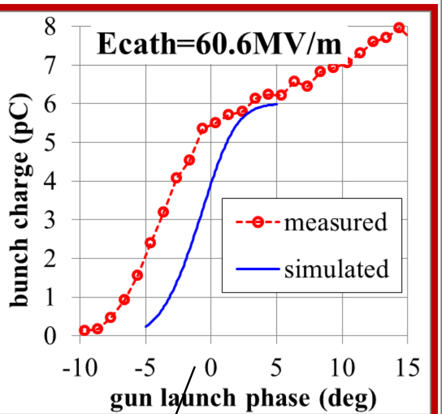

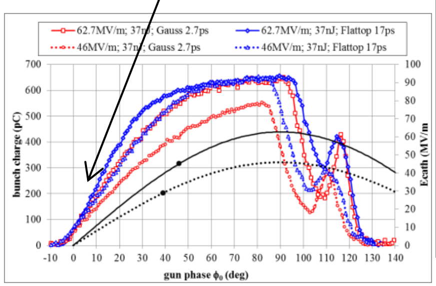

Measurements vs. Simulations

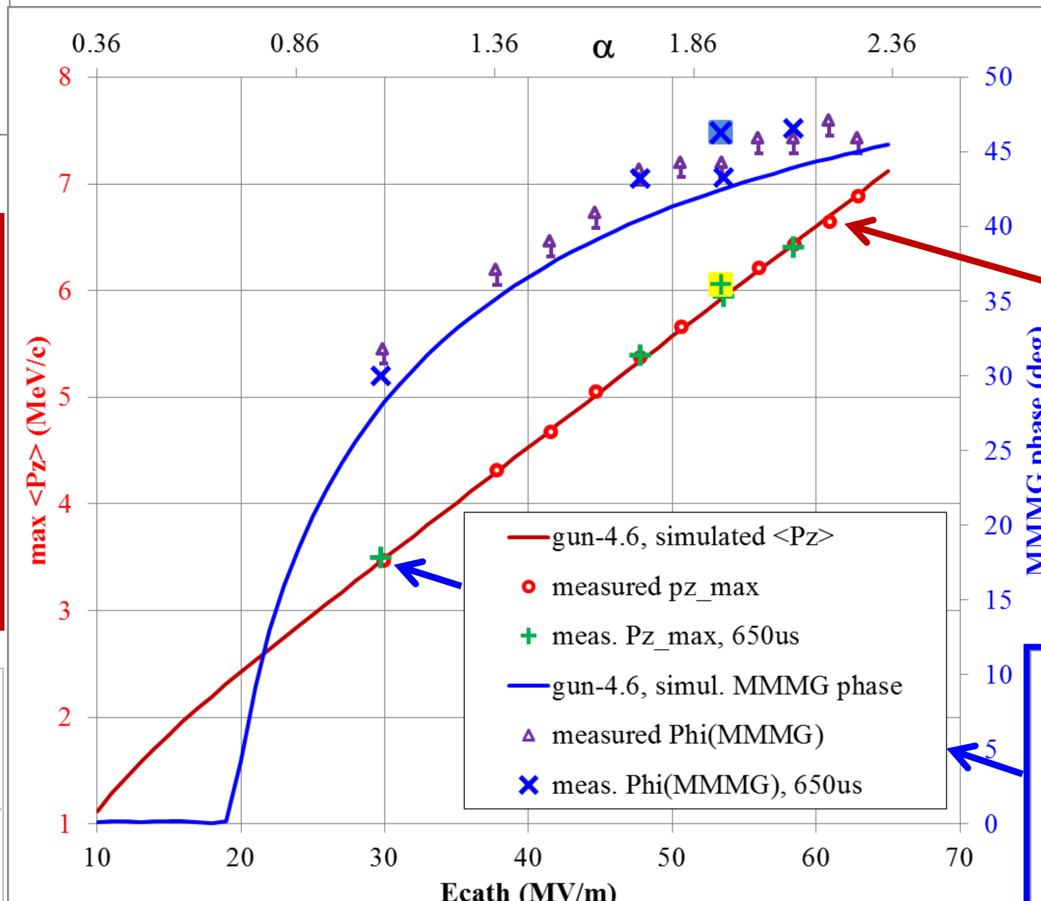

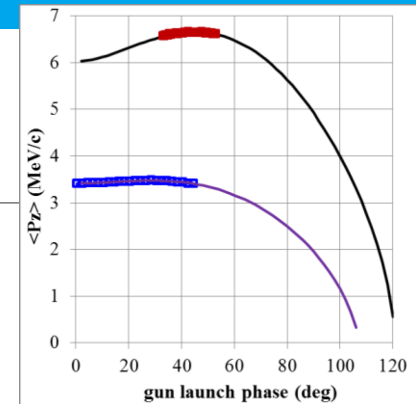

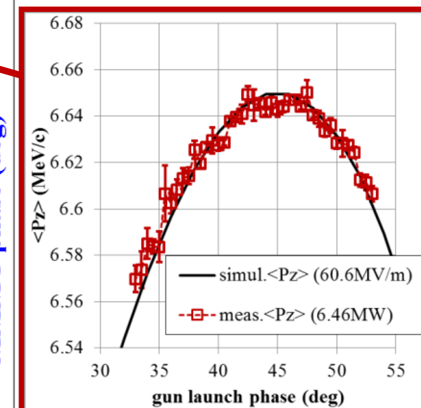

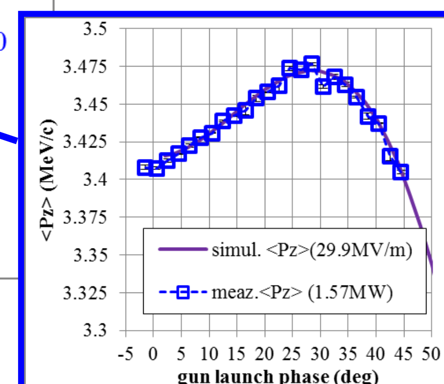

MMMG = Maximum Mean Momentum Gain

$$\alpha = \frac{eE_{cath}}{2mc^2k} \approx 0.047\frac{E_{cath}[MV/m]}{f[GHz]}$$

Zero-crossing phase determination

Still not understood: Zero-crossing phase ←→ MMMG phase ➔ 2-3 deg phase shift between measurements and simulations

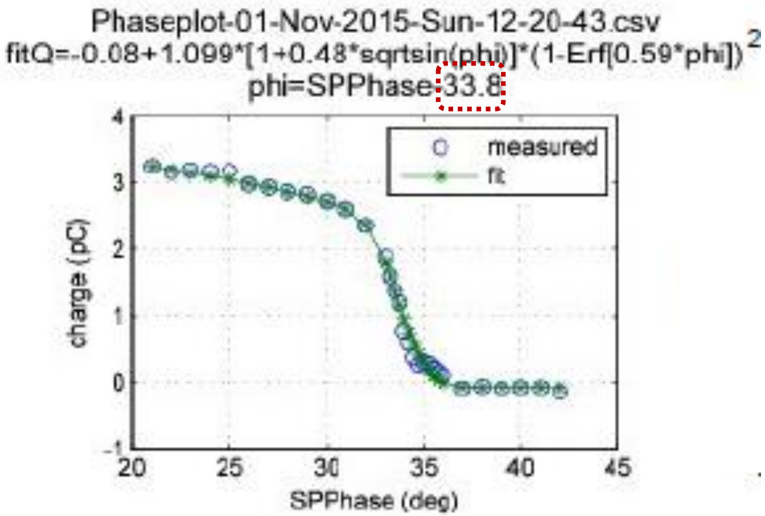

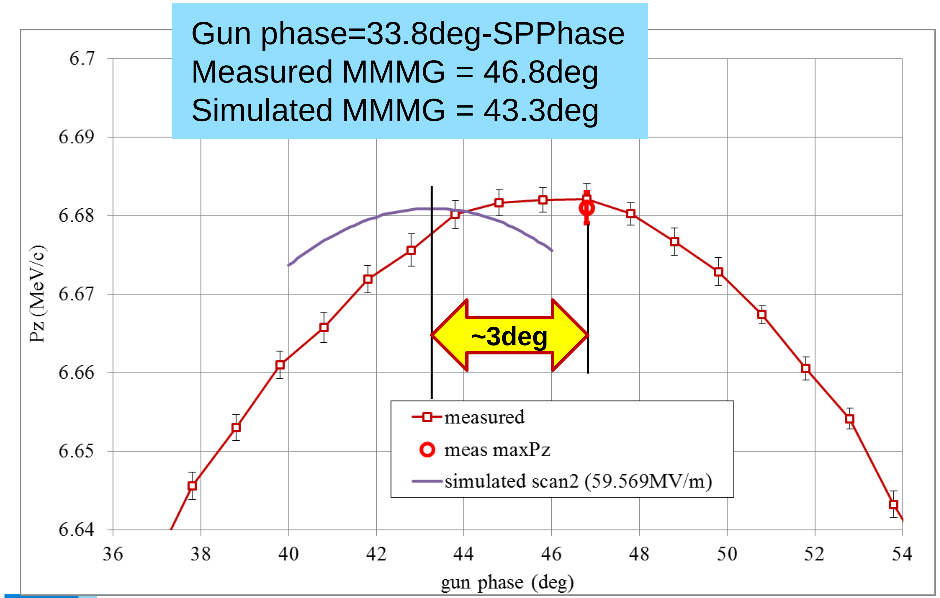

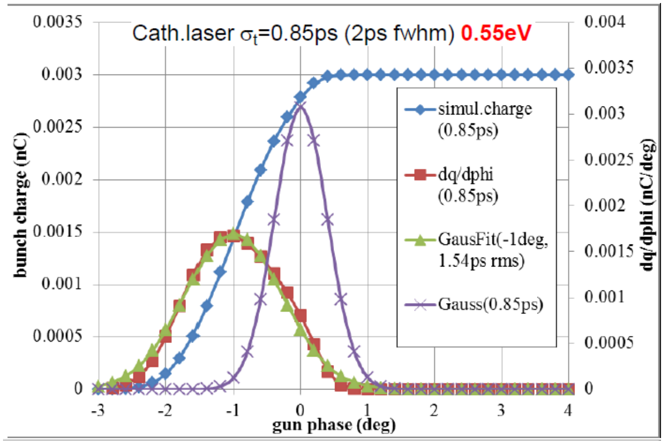

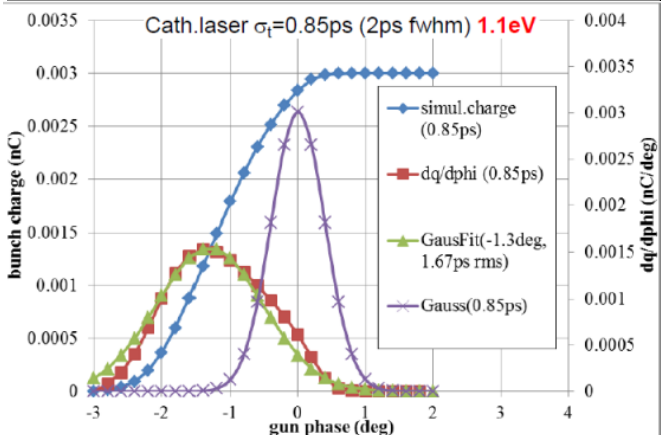

cathode laser		Ekin (eV)	delta phi	dq/dphi-Gauss.fit	fit-σ_t/σ_t
σ_t (ps)	fwhm (ps)		deg	fit-σ_t (ps)	
0.85	2	0.55	-1	1.54	1.81
0.85	2.6	1.1	-1.3	1.67	1.96

phase shift — widening

Another emission related topic at PITZ: slice energy spread

Main idea → δE measurements using TDS + HEDA2 dipole for various photo injector parameters (photocathode laser pulse temporal profiles, SC effect, etc.)

$$\delta_E^{measured} \approx \sqrt{\left(\delta_E^{real}\right)^2 + \left(\delta_E^{\beta}\right)^2 + \left(\delta_E^{TDS}\right)^2}$$

Still resolution on the slice energy spread seems to be a limiting factor:

Beam transverse size in the HEDA2 dipole (beta function)

TDS induced energy spread (estimated $\frac{d(\delta E)}{dSP(TDS)} \sim 3\,\frac{eV}{MV}$)

δE≈6.8 keV for TDS SP=0

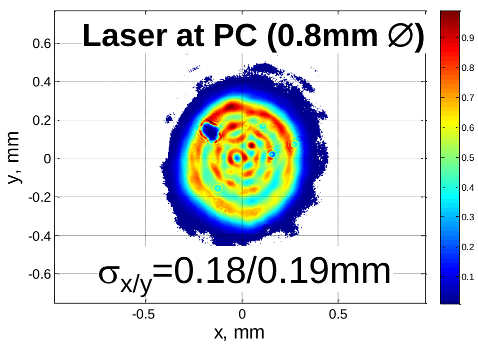

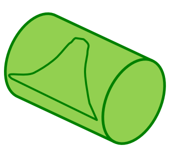

Longitudinal Phase Space (LPS) measurements: TDS SP scan in HEDA2 (**Long** Gaussian PC laser pulse, **11.5ps** FWHM)

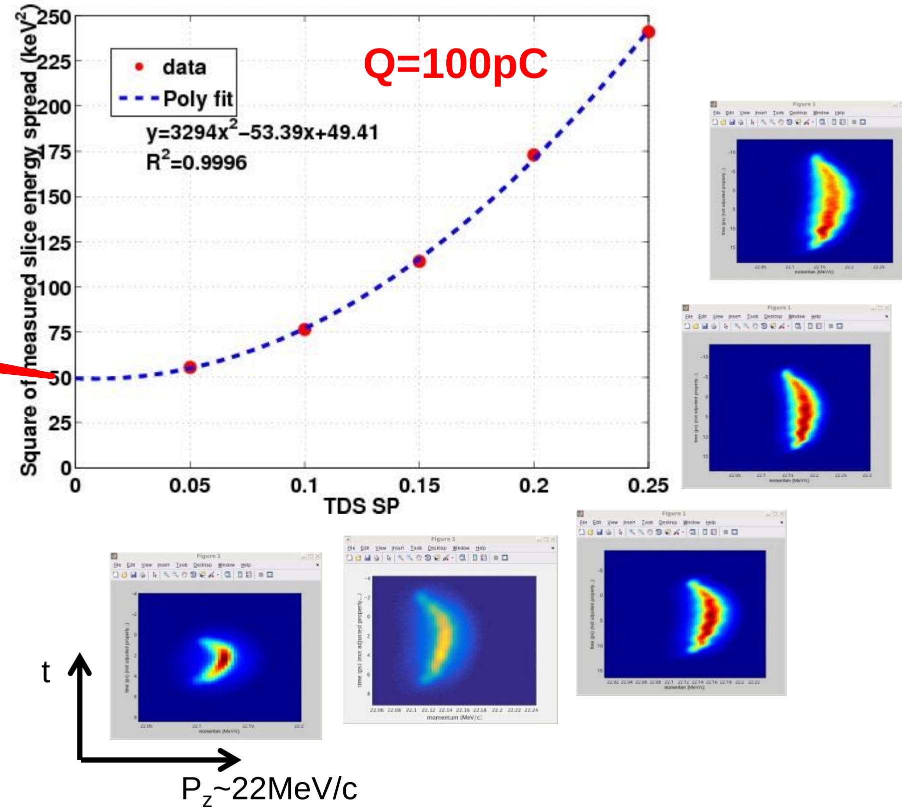

Similar measurements for **short** Gaussian (**2 ps** FWHM) PC pulses: **δE≈ 8.2 keV** for TDS SP=0

Slice energy spread: measurements vs. ASTRA simulations

ASTRA simulations:

- Q=100pC
- Gun+Booster → =measurements
- PC laser pulse parameters
  - Temporal: Gaussian (11.5 ps FWHM)
  - Transverse: Core+Halo, XYrms=0.186mm

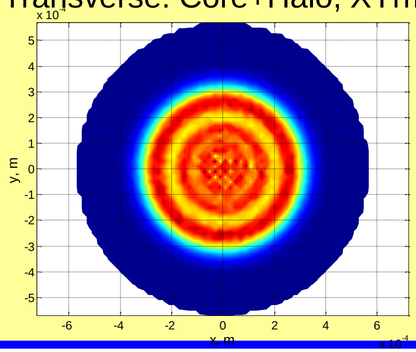

Simulated Long. Phase Space

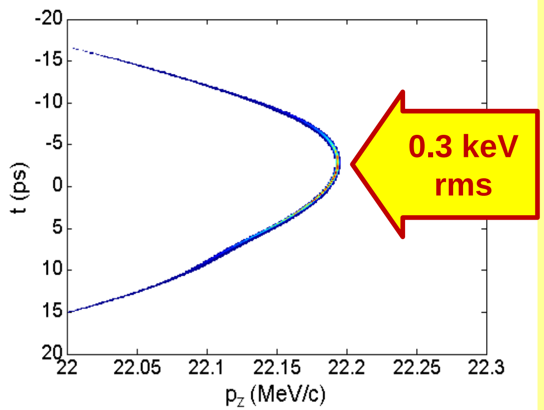

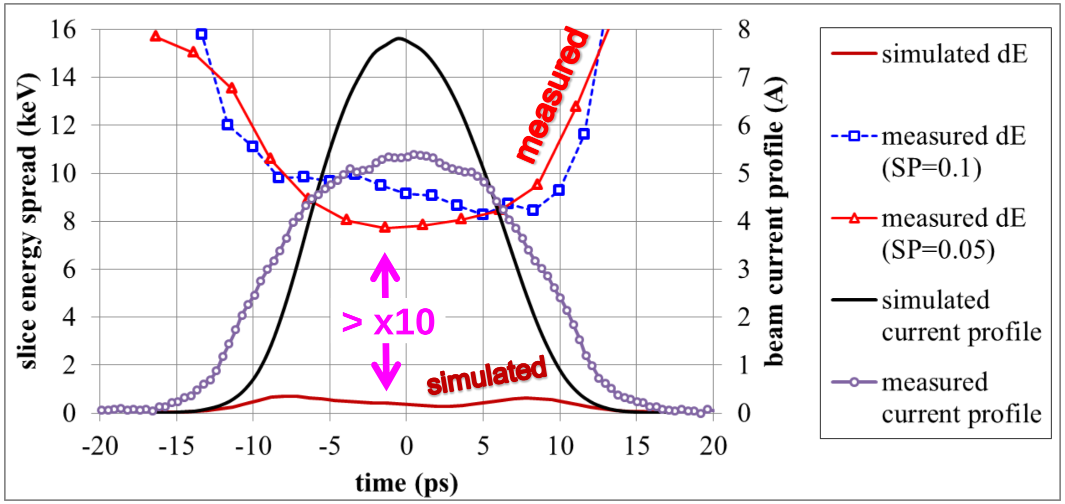

Measured Long. Phase Space

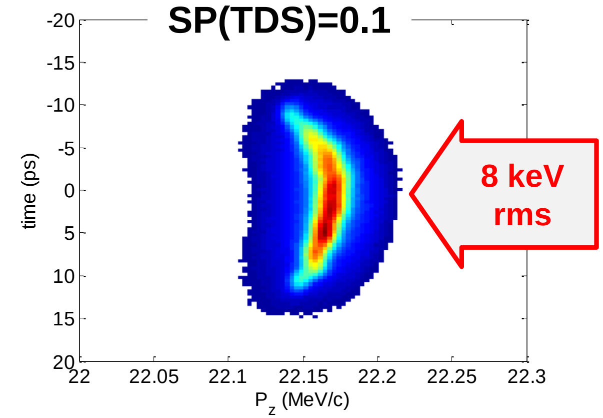

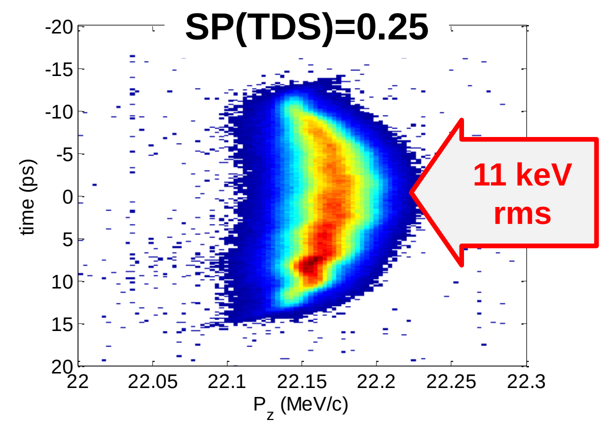

Conclusions and Outlook

- The Photo Injector Test facility at DESY in Zeuthen (PITZ) → high brightness electron sources for SASE FELs:
  - Low transverse emittance has been experimentally achieved
  - Still discrepancies between measured and simulated machine parameters
- Possible reasons of these discrepancies:
  - Imperfections (beam asymmetry) → compensation with gun quads
  - Photoemission
- Photoemission studies:
  - Best experimental emittance → **space charge dominated** photoemission
  - Generally: **$Q_{measured} > Q_{simulated}$(ideal case)**
  - Transverse **Core+Halo** model helps better for Gaussian than for flatttop temporal PC laser profiles
  - Could charge exceed be explained by secondary emission?
  - Still discrepancy measured-simulated phase spaces
  - "Phase offset" (1-3^o) measured-to-simulated zero-crossing RF phase is not well understood
  - Slice energy spread: $\delta E_{measured} >> \delta E_{simulated}$
- Outlook → new developments:
  - 3D ellipsoidal cathode laser pulses → experiments with electron beams

Back up slides

P_Z-modulation from the Gaussian PC laser pulses?

- E-beam momentum modulations observed in:
  LEDA (Pz~6.4MeV/c) and HEDA1 (Pz~22.1MeV/c)

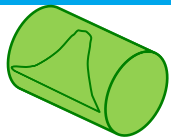

Temporal profile	FWHM
Long Gaussian	~11-11.5ps

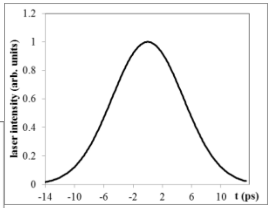

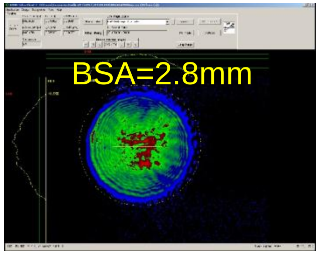

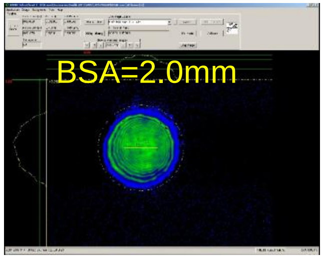

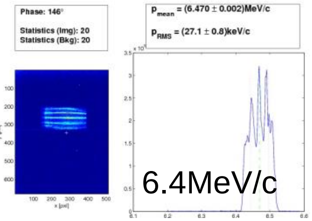

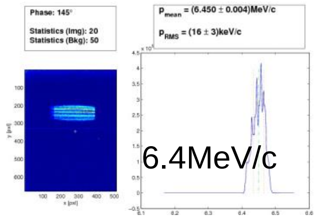

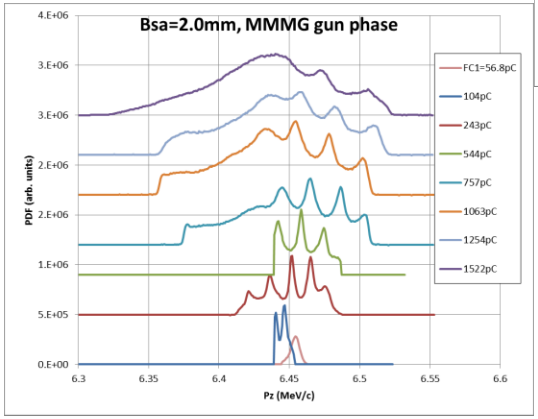

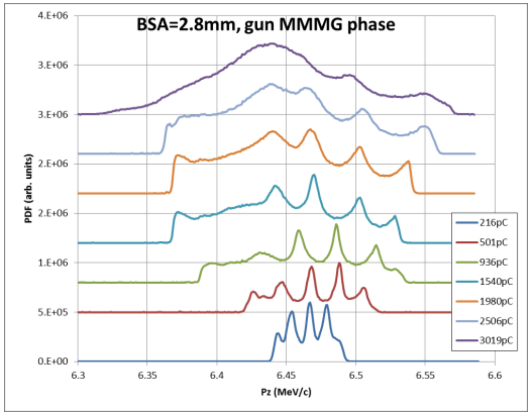

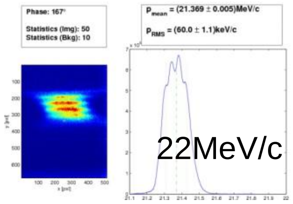

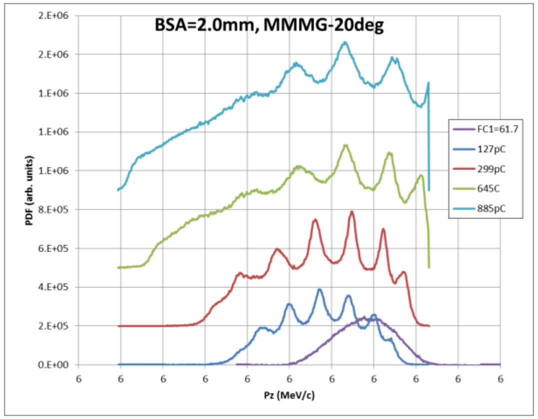

? Emitted charge → fields on surface that affects subsequent emissions → "oscillations induced by a sudden influx of charge can persist". Demonstration for Cu and Cs_3Sb using PIC code MICHELLE

- *J.J. Petillo et al., IEE trans. Electron Devices 52, 742 (2005)*
- *K.L. Jensen et al., J.Vac.Sci. Technol. 26 (2), 831 (2008)*

Might be related to the PC laser temporal profile → investigations are ongoing